Mathematical modeling of uranium and hydrocarbons recovery operations

IOP Conf. Series: Journal of Physics: Conf. Series **1479** (2020) 012055 doi:10.1088/1742-6596/1479/1/012055

Mathematical modeling of uranium and hydrocarbons recovery operations

O V Galtsev

Department of Information and Robotic Systems, Belgorod State National Research University, 85 Pobedy St., Belgorod, 308015, Russia

E-mail: galtsev_o@bsu.edu.ru

Abstract. The development of uranium and hydrocarbon deposits is a rather complex technological process consisting of several related sub-processes. One of them is the dissolution of solid soil by acid (in-situ leaching). The aim of this article is to model this process at the macroscopic level. The approach is based on the detailed consideration of fundamental laws of mechanics and chemistry at the pore scale. It is clear that the mathematical model obtained at the pore scale cannot be used in practical applications, but its simple and mathematically correct form allows further approximation by a system of homogenized equations. The dynamics of the liquid and the concentration of the reagent is described by a system of Darcy equations and the convection-diffusion equation respectively, obtained by homogenization the initial microscopic problem at the pore level. To solve the system of equations numerically, the method of finite differences on a uniformly spaced staggered grid is used. Temporal and spatial discretization of the equations is carried out. The results of numerical experiments are presented. The obtained results can help to analyse the active solution front motion in a porous medium and physical and chemical processes there.

1. Introduction

Real uranium deposits or hydrocarbon reservoirs are complicated geological heterogeneous bodies. Heterogeneity means that the property we are interested (porosity, saturation, etc.) in varies spatially. The suggested models have similar structures and principles. The differential equations in them are simply postulated. Often the effects of heterogeneities are generally not well accounted for at the planning stage of an operation. For example, the acid solution injected into the ground through wells may appears far from the intended location. Many other factors, like the concentration of injected acid, modes of injection acidic solutions, play an important role. An understanding of the movement of fluids and dissolution mechanism of rocks by acids within such heterogeneous porous media is therefore fundamental to uranium and petroleum production.

Currently the leaching of rocks is described by a large range of mathematical models at the macroscopic level (see [1–4], and references therein).

The differential equations in such models are simply postulated. As usual, the dynamics of the liquid is described by the Darcy system of filtration. The distribution of the reagent concentration is described by various modifications of the convection-diffusion equation, which contains an additional term of the chemical reaction.

In this article it is proposed to describe the process at the macroscopic level by the system of equations obtained using well-known homogenization methods [5] by performing a limit transition in the original microscopic (pore-scale) problem, since it is based on the laws of continuum mechanics (see [6]).

Dissolution of the rocks takes place exactly there. It changes the concentration of injected acid and the geometry of the pore space and creates the flow of products of chemical reactions into the pore space. All these principally important changes occur at the microscopic scale, corresponding to the mean size of pores or cracks in the rocks. The basic mechanism of the physical processes is concentrated on the unknown (free) boundary between the pore space and the solid skeleton but precisely this basic mechanism is not described in the proposed macroscopic models.

R. Burridge and J. B. Keller [7] and E. Sanchez-Palencia [8] were the first to state clearly that mathematical models for filtration and seismics must be rigorously derived from the microstructure.

To this end, one should:

(a) describe the physical process under consideration most precisely at the microscopic (pore) level (exact model),

(b) distinguish a set of small parameters,

(c) derive the macroscopic model as the asymptotic limit of the exact model.

Using models from Meirmanov [9] and methods developed for free boundary problems [10], homogenized analogs of microscopic equations are given here. He used generally accepted equations of continuum mechanics [11] and well-known chemical laws [12, 13]. The finite-difference approximation and numerical solution of equations are carried out.

2. Materials and methods

The physical process is considered in a bounded domain Ω of $\mathbb{R}^2$. The part S^+ of the boundary S of the domain Ω models the injecting wells, the part S^- of S models the pumping wells, and the part S^0 of S models the impermeable boundary of Ω (see figure 1).

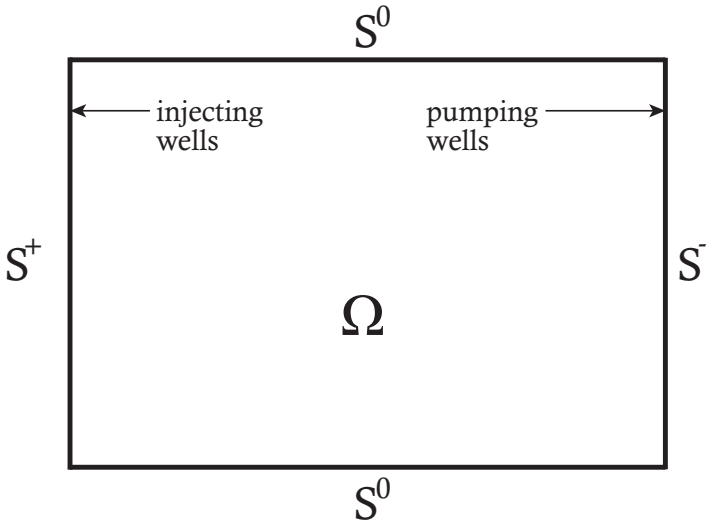

Figure 1. Domain under consideration for the macroscopic model.

In dimensionless variables

$$\mathbf{x} \to \frac{\mathbf{x}}{L},\ t \to \frac{t}{T},\ \mathbf{v} \to \frac{T}{L}\,\mathbf{v},\ p \to L\,g\,\rho^0\,p$$

the dynamics of the liquid are described by the Darcy law

$$\mathbf{v} = -\frac{1}{\mu}\,\mathbb{B}\cdot\nabla p \tag{1}$$

and nonhomogeneous continuity equation

$$\nabla\cdot\mathbf{v} = \delta\,\frac{\partial\, m}{\partial t} \tag{2}$$

for the velocity $\mathbf{v}$ and pressure p of pore liquid.

For the physical process of in-situ leaching Darcy's law could be taken to be the same, while the continuity equation must take into account the dissolution of the rocks by leaching.

The diffusion of reagent c is described by diffusion-convection equation

$$\frac{\partial}{\partial t}\left(m(c+\frac{1}{\gamma})\right) = \nabla\cdot(\alpha_c\,\mathbb{A}\cdot\nabla\, c - c\,\mathbf{v}) \tag{3}$$

for concentration c of the reagent.

In (1)–(3)

$$\alpha_c = \frac{D\,T}{W^2},\ \delta = \frac{(\rho_s-\rho_f)}{\rho_f},$$

μ is the fluid viscosity, ρ_s and ρ_f are dimensionless densities of the solid skeleton and the pore liquid correspondingly, correlated with the mean density of water ρ^0, W is the characteristic size of the domain under consideration, T is the characteristic time of the process, γ is some constant and D is a diffusion coefficient.

The problem is ended with the following boundary and initial conditions:

$$p = p^{\pm}(\mathbf{x},t),\ \mathbf{x}\in S^{\pm},\ \ t>0, \tag{4}$$

$$c = c^{+}(\mathbf{x},t),\ \mathbf{x}\in S^{+}, \tag{5}$$

$$\nabla c\cdot\mathbf{n} = 0,\ \mathbf{x}\in S^{-},\ \ t>0, \tag{6}$$

$$\nabla c\cdot\mathbf{n} = 0,\ \mathbf{v}\cdot\mathbf{n} = 0,\ \mathbf{x}\in S^{0},\ \ t>0, \tag{7}$$

$$c(\mathbf{x},0) = c_0(\mathbf{x}),\ \eta(\mathbf{x},0) = \eta_0(\mathbf{x})\ \mathbf{x}\in\Omega. \tag{8}$$

Here unknown function m (the porosity of pore space) is expressed by

$$m(\mathbf{x},t) = \int_Y \chi(\mathbf{x},t,\mathbf{y})dy,$$

and unknown matrices $\mathbb{A}$ and $\mathbb{B}$ are defined via unknown microstructure [9]:

$$\mathbb{B}(\mathbf{x},t) = \sum_{i=1}^{2}\int_{Y_f}\left(\mathbf{V}^{(i)}(\mathbf{x},t,\mathbf{y})\otimes\mathbf{e}_i\right)\cdot\mathbf{e}_i dy,$$

$$\triangle_y\mathbf{V}^{(i)} - \nabla\,\Pi^{(i)} + \mathbf{e}_i = 0,\ \nabla_y\cdot\mathbf{V}^{(i)} = 0,\ \ \mathbf{y}\in Y_f(\mathbf{x},t), \tag{9}$$

$$\mathbf{V}^{(i)} = 0, \;\; \mathbf{y} \in \eta(\mathbf{x}, t);$$

$$\mathbb{A}(\mathbf{x}, t) = m\,\mathbb{I} + \int_{Y_f} \mathbb{D}(\mathbf{x}, t, \mathbf{y}) dy, \;\; \mathbb{I} = \begin{pmatrix} 1 & 0 \\ 0 & 1 \end{pmatrix}, \tag{10}$$

$$\mathbb{D}(\mathbf{x}, t, \mathbf{y}) = \sum_{i=1}^{2} \nabla_y C^{(i)}(\mathbf{x}, t, \mathbf{y}) \otimes \mathbf{e}_i, \tag{11}$$

where $\Pi^{(i)}$ is the pressure for some auxiliary problem, $(\mathbf{e}_1, \mathbf{e}_2)$ is a standard cartesian basis and the matrix $\mathbb{B} = \mathbf{a} \otimes \mathbf{b}$ is defined as $\mathbb{B} \cdot \mathbf{c} = \mathbf{a}(\mathbf{b} \cdot \mathbf{c})$.

The 1-periodic in $\mathbf{y}$ functions $C^{(i)}(\mathbf{x}, t, \mathbf{y})$, $i = 1, 2$ at each point $\mathbf{x} \in \Omega$ for $t > 0$ solve the periodic boundary-value problem

$$\triangle_y C^{(i)} = 0, \;\; \mathbf{y} \in Y_f(\mathbf{x}, t), \tag{12}$$

$$(\mathbf{e}_i + \nabla_y C^{(i)}) \cdot \mathbf{n} = 0, \;\; \mathbf{y} \in \eta(\mathbf{x}, t) = \partial\, Y_f(\mathbf{x}, t) \tag{13}$$

in the unknown subdomain $Y_f(\mathbf{x}, t) \subset Y$ of the unit square Y (see figure 2).

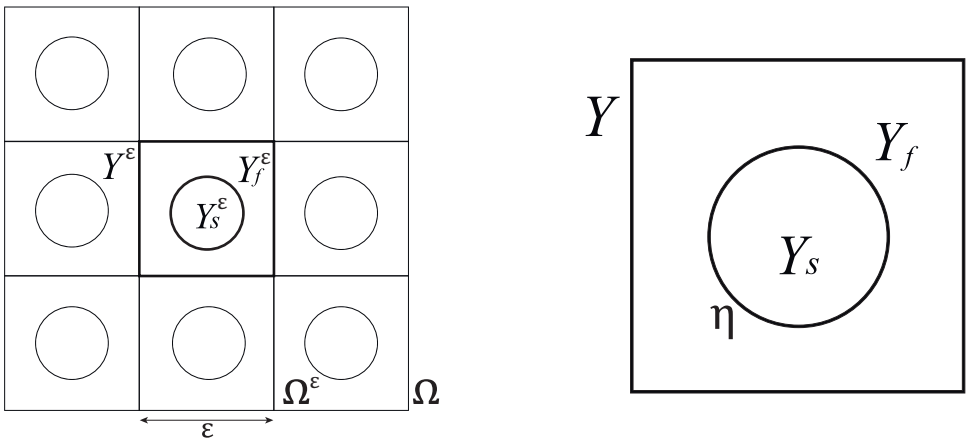

Figure 2. Domain Ω by periodic repetition of a porous medium Ω^ε represented by a unit cell Y.

In (13) $\mathbf{n}$ is the unit normal vector to the boundary $\eta(\mathbf{x}, t)$.

The behavior of the unknown (free) boundary $\eta(\mathbf{x}, t)$ of domain $Y_f(\mathbf{x}, t)$ is governed by the following equation

$$K_n(\mathbf{x}, \mathbf{y}, t) = \beta\, \gamma\, c(\mathbf{x}, t), \tag{14}$$

where $K_n(\mathbf{x}, \mathbf{y}, t)$ is the velocity of the boundary $\eta(\mathbf{x}, t)$ at the point $\mathbf{y} \in \eta(\mathbf{x}, t)$ in the outward to Y_f normal direction $\mathbf{n}$ to the boundary $\eta(\mathbf{x}, t)$.

Any physical problem contains dimensionless parameters (criteria), which somehow characterize the problem. Some of them might be small, some of them might be large, but all of them are fixed. On the other hand, when the physical problem has already been formulated as a mathematical problem, we may consider a family of mathematical problems with a variable small parameter and look for approximate mathematical models (homogenization), when this small parameter goes to zero.

Thus macroscopic equations (1)–(3), (14) for $\mathbf{v}(\mathbf{x}, t) = \int_Y \mathbf{V}(\mathbf{x}, t, \mathbf{y}) dy$, $p(x, t)$, $c(x, t)$ and unknown coefficients are obtained after the limiting procedure as the small parameter ε goes to

zero (two-scale expansion method) in the microscopic problem described in [6]. The following assumptions and well-known mathematical formulas were used here:

$$\mathbf{v}^{\varepsilon}(\mathbf{x},t) = \mathbf{V}(\mathbf{x},t,\frac{\mathbf{x}}{\varepsilon}) + o(\varepsilon),$$

$$p^{\varepsilon}(\mathbf{x},t) = p(\mathbf{x},t) + o(\varepsilon),$$

$$c^{\varepsilon}(\mathbf{x},t) = c(\mathbf{x},t) + o(\varepsilon),\ \nabla c^{\varepsilon}(\mathbf{x},t) = \nabla c(\mathbf{x},t) + \nabla_y C(\mathbf{x},t,\frac{\mathbf{x}}{\varepsilon}) + o(\varepsilon),$$

$$\lim_{\varepsilon\to 0}\int_Y U(\mathbf{x},t,\frac{\mathbf{x}}{\varepsilon})dxdt = \int_Q \Big(\int_Y U(\mathbf{x},t,\mathbf{y})dy\Big)dxdt,$$

where $\varepsilon = \frac{l}{L}$ is a dimensionless pore size, $\chi(\mathbf{x},\mathbf{y},t)$ and $U(\mathbf{x},t,\mathbf{y})$ are 1-periodic in $\mathbf{y} \in Y = (0,1)^2 \subset \mathbb{R}^2$ functions. This limit depends on the differential properties of $\{\mathbf{v}^{\varepsilon},\ p^{\varepsilon},\ c^{\varepsilon}\}$.

Be reminded that this problem (1)–(13) has been obtained for the given function $\chi(\mathbf{y},t)$.

To solve the problem (1)–(8) one may use the fixed-point theorem. For example, for given $\chi(\mathbf{y},t)$ find solution $\{\mathbf{v},\ p,\ c\}$ to the problem (1)–(13), and after that use the condition (14) as an equation for the function $\chi(\mathbf{y},t)$.

2.1. Finite-difference approximation

The area described above was used as the calculated one (see figure 1). The numerical modeling is carried out by the finite differences method. First of all, the integration area is covered by a fixed (Eulerian) grid with rectangular cells with sides Δx and Δy [14]. The values of the integers i (along x) and j (along y) denote the center of the cell (see figure 3).

$$\Omega = \begin{pmatrix} x_{(i+1/2)} = (i+1/2)\Delta x,\ \Delta x > 0;\ i = 0,1,...,N;\ (N+1)\Delta x = X_{max} \\ x_{(j+1/2)} = (j+1/2)\Delta y,\ \Delta y > 0;\ j = 0,1,...,M;\ (M+1)\Delta y = Y_{max} \end{pmatrix}$$

where N, M are the number of grid cells.

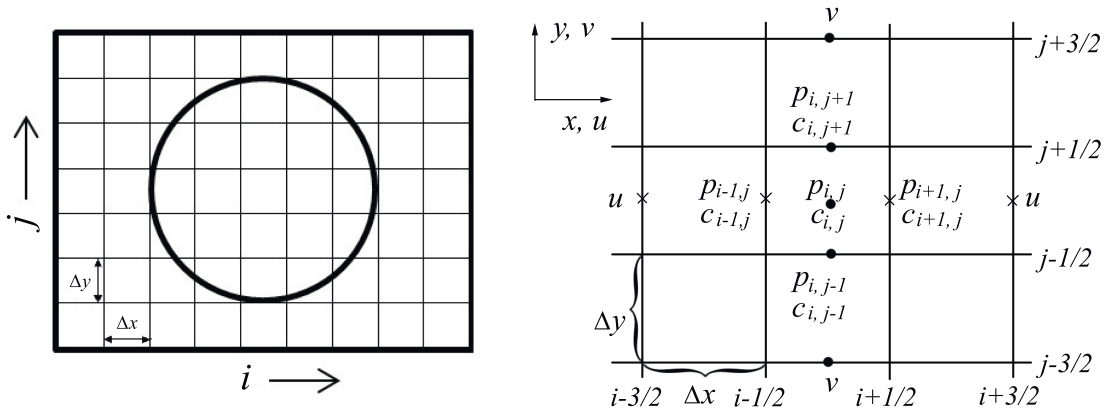

Figure 3. Grid template.

In our case, we used a grid with a "staggered" arrangement of nodes (see figure 3). Thus, a separate cell acts as a separate element of the medium with the pressure p_{ij} characterizing it and the concentration c_{ij} in the center.

This explicit technique uses the following approximations hereinafter [15],

$$\frac{\partial c}{\partial t} \backsimeq \frac{c_{i,j}^{d+1} - c_i^d}{\Delta t},\ \frac{\partial u}{\partial x} \backsimeq \frac{u_{i+\frac{1}{2},j}^d - u_{i-\frac{1}{2},j}^d}{\Delta x},\ \frac{\partial v}{\partial y} \backsimeq \frac{v_{i,j+\frac{1}{2}}^d - v_{i,j-\frac{1}{2}}^d}{\Delta y}, \tag{15}$$

$$\frac{\partial^2 c}{\partial x \partial y} = \frac{1}{2\Delta y}\left(\frac{c_{i+\frac{1}{2},j+\frac{1}{2}} - c_{i-\frac{1}{2},j+\frac{1}{2}}}{2\Delta x} - \frac{c_{i+\frac{1}{2},j-\frac{1}{2}} - c_{i-\frac{1}{2},j-\frac{1}{2}}}{2\Delta x}\right), \tag{16}$$

$$\frac{\partial^2 c}{\partial x^2} = \frac{c_{i+\frac{3}{2},j} - 2\,c_{i+\frac{1}{2},j} + c_{i-\frac{1}{2},j}}{\Delta x^2},\ \frac{\partial^2 c}{\partial y^2} = \frac{c_{i,j+\frac{3}{2}} - 2c_{i,j+\frac{1}{2}} + c_{i,j-\frac{1}{2}}}{\Delta y^2}, \tag{17}$$

where $\Delta t = t^d - t^{d-1}$, d is a time step. Values with fractional indices are calculated as the arithmetic mean.

This representation allows us to approximate partial differential equations with the second highest spatial variable order of accuracy, where the error has the order of accuracy $O(\Delta t, h^2)$ ($h = \max(\delta x, \Delta y)$).

Solving the system of equations (9)–(13) obtain matrices $\mathbb{A}$ and $\mathbb{B}$

$$\mathbb{A} = \begin{pmatrix} a_{11} & a_{12} \\ a_{21} & a_{22} \end{pmatrix},\ \mathbb{B} = \begin{pmatrix} b_{11} & b_{12} \\ b_{21} & b_{22} \end{pmatrix}. \tag{18}$$

The finite difference approximation of equation (1) componentwise takes the form:

$$u_{i,j}^{d+1} = -\frac{1}{\mu}\left(\frac{b_{11}}{\Delta x}(p^d_{i+\frac{1}{2},j} - p^d_{i-\frac{1}{2},j}) + \frac{b_{12}}{\Delta y}(p^d_{i,j+\frac{1}{2}} - p^d_{i,j-\frac{1}{2}})\right), \tag{19}$$

$$v_{i,j}^{d+1} = -\frac{1}{\mu}\left(\frac{b_{21}}{\Delta x}(p^d_{i+\frac{1}{2},j} - p^d_{i-\frac{1}{2},j}) + \frac{b_{22}}{\Delta y}(p^d_{i,j+\frac{1}{2}} - p^d_{i,j-\frac{1}{2}})\right). \tag{20}$$

The finite difference analogue to equation (2):

$$m_{i,j}^{d+1} = m_{i,j}^d \frac{\Delta t}{\mu\delta}\left(\frac{b_{11}}{\Delta x^2}(p^d_{i+\frac{3}{2},j} - 2\,p^d_{i+\frac{1}{2},j} + p^d_{i-\frac{1}{2},j}) + \right.$$
$$\left. \frac{b_{22}}{\Delta y^2}(p^d_{i,j+\frac{3}{2}} - 2\,p^d_{i,j+\frac{1}{2}} + p^d_{i,j-\frac{1}{2}}) + \frac{\omega}{2}(b_{12} + b_{21})\right). \tag{21}$$

Finally the finite difference analogue to equation (3):

$$c_{i,j}^{d+1} = c_{i,j}^d + \frac{\Delta t}{m_{i,j}^{d+1}} \times \left[\alpha_c\left\{\frac{\eta}{2}(a_{12} + a_{21}) + \frac{a_{11}}{\Delta x^2}\left(c^d_{i+\frac{3}{2},j} - 2\,c^d_{i+\frac{1}{2},j} + c^d_{i-\frac{1}{2},j}\right) + \right.\right.$$
$$\frac{a_{22}}{\Delta y^2}\left(c^d_{i,j+\frac{3}{2}} - 2\,c^d_{,ji+\frac{1}{2}} + c^d_{i,j-\frac{1}{2}}\right)\Big\} + \Big\{\frac{b_{11}}{\Delta x^2}\left(p^d_{i+\frac{3}{2},j} - 2\,p^d_{i+\frac{1}{2},j} + p^d_{i-\frac{1}{2},j}\right) +$$
$$\frac{b_{22}}{\Delta y^2}\left(p^d_{i,j+\frac{3}{2}} - 2\,p^d_{i,j+\frac{1}{2}} + p^d_{i,j-\frac{1}{2}}\right) + \frac{\omega}{2}(b_{12} + b_{21})\Big\} \times \frac{1}{\delta\mu}\left(c^d_{i,j} + \frac{1}{\gamma}\right) +$$
$$c^d_{i,j}\left\{\frac{b_{11}}{\Delta x^2}\left(p^d_{i+\frac{3}{2},j} - 2\,p^d_{i+\frac{1}{2},j} + p^d_{i-\frac{1}{2},j}\right) + \frac{b_{22}}{\Delta y^2}\left(p^d_{i,j+\frac{3}{2}} - 2\,p^d_{i,j+\frac{1}{2}} + p^d_{i,j-\frac{1}{2}}\right) + \right.$$
$$\left.\frac{\omega}{2}(b_{12} + b_{21})\right\} + \frac{c^d_{i+\frac{1}{2},j} - c^d_{i-\frac{1}{2},j}}{\Delta x}\left\{\frac{b_{11}}{\Delta x}\left(p^d_{i+\frac{1}{2},j} - p^d_{i-\frac{1}{2},j}\right) + \frac{b_{12}}{\Delta x}\left(p^d_{i,j+\frac{1}{2}} - p^d_{i,j-\frac{1}{2}}\right)\right\} +$$
$$\frac{c^d_{i,j+\frac{1}{2}} - c^d_{i,j-\frac{1}{2}}}{\Delta y}\left\{\frac{b_{21}}{\Delta x}\left(p^d_{i+\frac{1}{2},j} - p^d_{i-\frac{1}{2},j}\right) + \frac{b_{22}}{\Delta y}\left(p^d_{i,j+\frac{1}{2}} - p^d_{i,j-\frac{1}{2}}\right)\right\} \Big/$$
$$\left(\frac{c^d_{i+\frac{3}{2},j} - 2\,c^d_{i+\frac{1}{2},j} + c^d_{i-\frac{1}{2},j}}{\Delta x^2} + \frac{c^d_{i,j+\frac{3}{2}} - 2\,c^d_{i,j+\frac{1}{2}} + c^d_{i,j-\frac{1}{2}}}{\Delta y^2}\right)^{\frac{1}{2}} \times \left(\omega\,(b_{11}b_{12} + b_{21}b_{22}) + \right.$$
$$\left.\left.\frac{b_{11}^2 + b_{21}^2}{\Delta x^2}\left(p^d_{i+\frac{3}{2},j} - 2\,p^d_{i+\frac{1}{2},j} + p^d_{i-\frac{1}{2},j}\right) + \frac{b_{12}^2 + b_{22}^2}{\Delta y^2}\left(p^d_{i,j+\frac{3}{2}} - 2\,p^d_{i,j+\frac{1}{2}} + p^d_{i,j-\frac{1}{2}}\right)\right)^{\frac{1}{2}}\right]. \tag{22}$$

Using the following equation we find the pressure field:

$$p_{i,j}^{d+1} = \frac{u_{i+1/2,j}^{d+1} - u_{i-1/2,j}^{d+1}}{\Delta x} + \frac{v_{i,j+1/2}^{d+1} - v_{i,j-1/2}^{d+1}}{\Delta y} - (b_{11} + b_{12}) \frac{p_{i+\frac{1}{2},j}^{d} - p_{i-\frac{1}{2},j}^{d}}{\Delta x} - (b_{21} + b_{22}) \frac{p_{i,j+\frac{1}{2}}^{d} - p_{i,j-\frac{1}{2}}^{d}}{\Delta y}. \quad (23)$$

In (21) and (22)

$$\omega = \frac{p_{i+\frac{1}{2},j+\frac{1}{2}}^{d} - p_{i-\frac{1}{2},j+\frac{1}{2}}^{d} - p_{i+\frac{1}{2},j-\frac{1}{2}}^{d} + p_{i-\frac{1}{2},j-\frac{1}{2}}^{d}}{2\Delta x \Delta y},$$

$$\eta = \frac{c_{i+\frac{1}{2},j+\frac{1}{2}}^{d} - c_{i-\frac{1}{2},j+\frac{1}{2}}^{d} - c_{i+\frac{1}{2},j-\frac{1}{2}}^{d} + c_{i-\frac{1}{2},j-\frac{1}{2}}^{d}}{2\Delta x \Delta y}.$$

At the boundaries S^0 the adhesion and impermeability conditions are satisfied

$$v_{-\frac{1}{2},j+\frac{1}{2}}^{d} = 0,$$

$$u_{i-\frac{1}{2},j}^{d} = 0.$$

The solution of the initial system of equations is possible when the following criterion is met

$$\max \left| \frac{u^{d+1} - u^{d}}{u^{d+1}} \right| \leq \varsigma,$$

where ς is the error value.

2.2. Numerical results

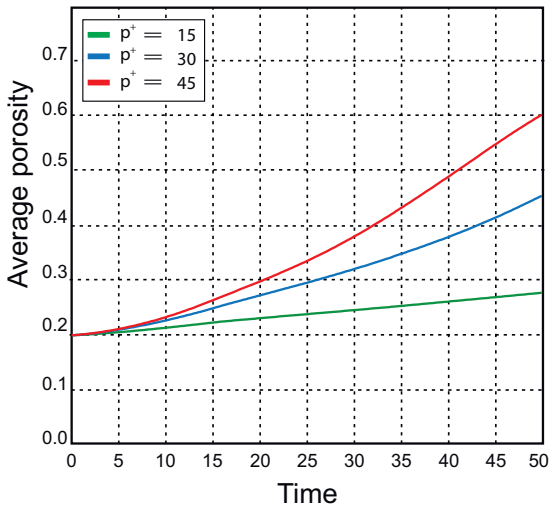

Figure 4. Average porosity for different values of p^+.

The numerical solution for macroscopic mathematical model describing the interaction of active impurity was obtained.

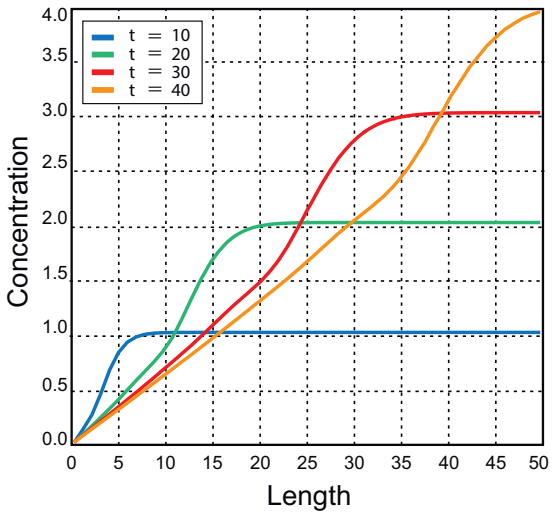

Figure 5. Concentration distribution of the acid for different dimensionless t.

To simplify the numerical calculations, suppose that the matrices $\mathbb{A}$ and $\mathbb{B}$ are symmetric. At the initial moment of time, the porosity of the medium is uniformly distributed over the entire area.

Calculations of modeling the impurity concentration for different time for the following parameters of the model

$$\gamma = 1,\ \delta = 1,\ \alpha_c = 0.4,\ W = 50,\ H = 25,\ T = 50$$

and for different values of c^+, p^+ and t are presented in figures 4–7.

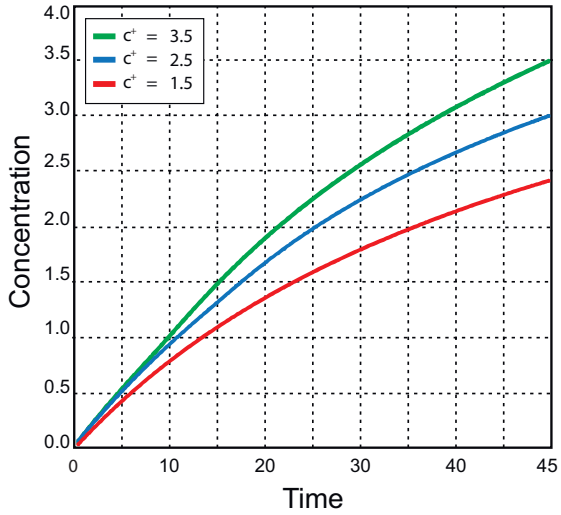

Figure 6. Concentration of the acid at the pumping wells for different c^+.

For $c^+ = 4$, $p^- = 0$ and starting $m_0 = 0.2$ we calculate the average porosity for different values of $p^+ = [15; 30; 45]$ at the injecting wells (see figure 4).

Figure 5 in the computational domain for different moments of dimensionless time t=[10;20;30;40] presents the results of the distribution of the reagent concentration .

Numerical calculations the reagent concentration at the pumping wells for different values of $c^+ = [1.5; 2.5; 3.5]$ and for $p^+ = 100$, $p^- = 0$, $m = 0.2$ shows us a monotonic increase in the products of a chemical reaction during underground leaching (see figure 6).

Figure 7 shows the acid diffusion for different moments of time at a constant acid concentration corresponding to $c^+ = 4$, $p^- = 0$.

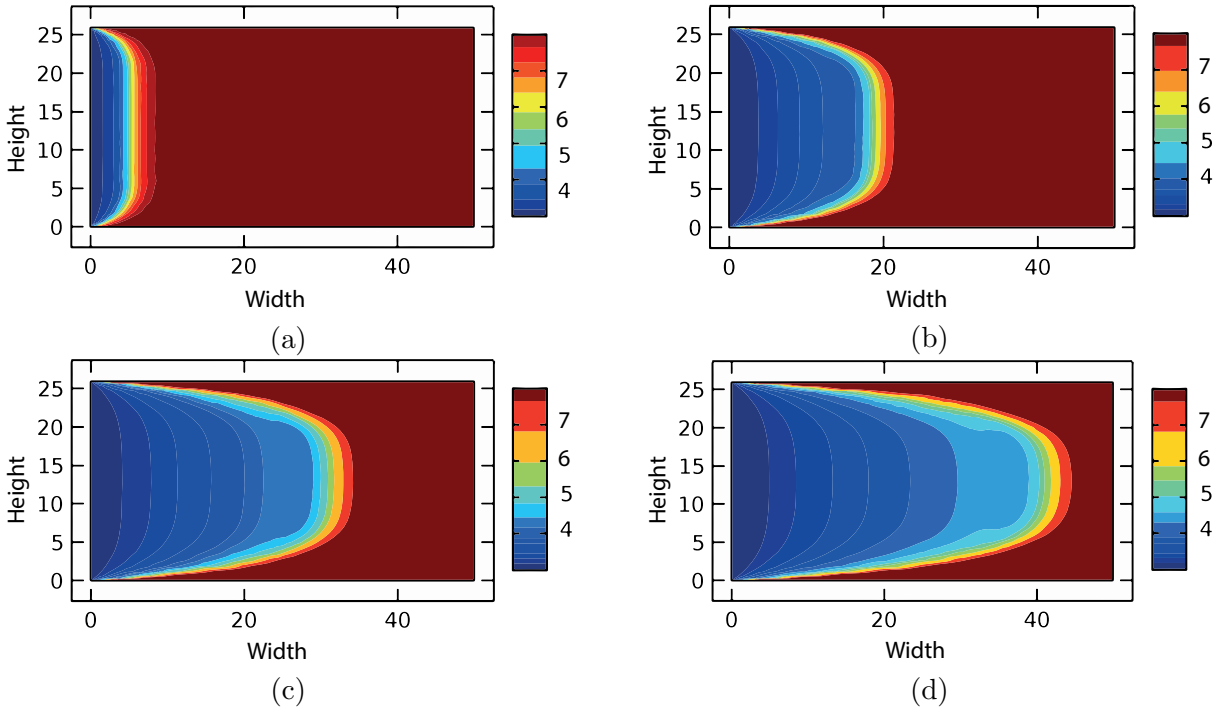

Figure 7. Acid concentration at different dimensionless time moments: a) t = 10, b) t = 20, c) t = 26, d) t = 30.

Acknowledgments
The reported study was funded by RFBR according to the research project No 18-31-00042.

Conclusion

In this paper we considered a macroscopic mathematical model, which describes the interaction of an acid in porous medium. Some numerical simulations show the distinctive features of the model. For example, the concentrations of reagent and products of chemical reactions in the pumping wells (correspondingly) depend monotonically on the concentration c^+ at the given boundary. The rate of outflow of fluid from the free boundary is proportional to the concentration of the acid and grows when this concentration increases. The domination of outflow of fluid from the free boundary reduces the diffusion of reagent, and leads to a decrease of reagent concentration at the free boundary. In turn, this implies a decrease of the outflow of fluid from the free boundary and a domination of the diffusion of the acid inward from the free boundary. The growth of reagent diffusion toward the free boundary leads to an increase of reagent concentration at the free boundary and so on (see figures 4–7). Changing constants γ and δ it is possible to achieve an acceptable match the simulation results to experimental data.

References

[1] Golfier F *et al.* 2002 *J. Fluid Mech.* **457** 213
[2] Kalia N and Balakotaiah V 2009 *Chem. Eng. Sci.* **64** 376
[3] Cohen C *et al.* 2008 *Chem. Eng. Sci.* **63** 3088
[4] M Panga M Z and Balakotaiah V 2005 *A.I.Ch.E.Journal* **51** 3231
[5] Nguetseng G 1990 *SIAM J. Math. Anal.* **21** 1394
[6] Galtsev O and Galtseva O 2018 *International journal of engineering and technology(uae)* **7** 5
[7] Burridge R and Keller J 1981 *J. Acoust. Soc. Am.* **70** 1140
[8] Sanchez-Palencia E 1980 *Non-Homogeneous Media and Vibration Theory* (Berlin: Springer)
[9] Meirmanov A 2013 *Mathematical models for poroelastic flows* (Paris: Atlantis Press)
[10] Meirmanov A 1992 *The Stefan Problem* (Berlin: Walter de Gruyter)
[11] Malvern L 1992 *Introduction to Mechanics of a Continuum Medium* (New York: Prentice-Hall)
[12] Brady P and House W 1996 *Phys. Chem. Min.* 226
[13] Kenneth W *et al.* 2014 *Chemistry* 10th ed (Brooks: Belmont)
[14] Virieux J 1986 *Geophysics* **51** 889
[15] Belotserkovskiy O 1984 *Numerical modeling in continuum mechanics* (Moscow: Nauka)